DFIG-Based Wind Turbine with Shunt Active Power Filter Controlled by Double Nonlinear Predictive Controller

Abderrahmane El Kachani, El Mahjoub Chakir, Anass Ait Laachir, Abdelhamid Niaaniaa, Jamal Zerouaoui, Tarik Jarou

Abstract—This paper presents a wind turbine based on the doubly fed induction generator (DFIG) connected to the utility grid through a shunt active power filter (SAPF). The whole system is controlled by a double nonlinear predictive controller (DNPC). A Taylor series expansion is used to predict the outputs of the system. The control law is calculated by optimization of the cost function. The first nonlinear predictive controller (NPC) is designed to ensure the high performance tracking of the rotor speed and regulate the rotor current of the DFIG, while the second one is designed to control the SAPF in order to compensate the harmonic produces by the three-phase diode bridge supplied by a passive circuit (rd, Ld). As a result, we obtain sinusoidal waveforms of the stator voltage and stator current. The proposed nonlinear predictive controllers (NPCs) are validated via simulation on a 1.5 MW DFIG-based wind turbine connected to an SAPF. The results obtained appear to be satisfactory and promising.

Keywords—Wind power, doubly fed induction generator, shunt active power filter, double nonlinear predictive controller.

I. INTRODUCTION

IN recent years, there has been an evolution of the production of electricity based on wind power. This energy source has been developed particularly in light of the diversity of exploitable zones and a relatively attractive cost [1].

Currently, most wind turbines are equipped with DFIG, due to several advantages: variable speed operation (± 30% around the synchronism speed), active and reactive power independent control. Thus, improving the quality of power and lower converter cost [1].

As a wind energy conversion system technology that still in progress, several control techniques are developed in terms of wind turbine connection to the utility grid and filtering of this one. The connection of the SAPF between the DFIG-based wind turbine and utility grid has received much attention in recent years due to the use of the power electronic equipment

A. El Kachani is with LHESIR Laboratory, Department of Physics at Ibn Tofail University, Kenitra, B.P 242, Morocco (phone: +212665780527; e-mail: elkachani.abderrahmane@gmail.com).

A. Ait Laachir, A. Niaaniaa and J. Zerouaoui are with LHESIR Laboratory, Department of Physics, Ibn Tofail University, Kenitra, B.P 242, Morocco, (e-mail: anass.aitlaachir@gmail.com, niaaniaa.abdelhamid@gmail.com, J.zerouaoui@yahoo.fr).

E. Chakir is with LHESIR Laboratory, Ibn Tofail University, Kenitra, B.P 242, Morocco (e-mail: mahchakir@yahoo.fr).

T. Jarou is with LHESIR Laboratory, Department of Electrical Engineering, ENSA, Ibn Tofail University, Kenitra, B.P 242, Morocco (e-mail: tarik.jarou@hotmail.com).

and electric arc loads. The electromagnetic disturbances are proliferating in public and industrial electrical installations. Indeed, it is important that the wind turbine must ensure the energy quality.

As we can see in Fig. 1, the three-phase stator winding of DFIG is connected to the grid. While the three-phase rotor winding is connected to AC-DC-AC converters. The rotor side converter (RSC) controls active and reactive power between stator of DFIG and grid.

The DFIG is subject to many constraints, such as the effects of parametric uncertainties (due to overheating, saturation ...) and the perturbation caused by the speed variation, these problems could divert the system of its optimal operation. This is why the control should be concerned about the robustness and performance [2]. For that, we referred to the use of the model predictive control (MPC). This MPC has received much attention and constitutes a very active field of research in recent years. It is based on the optimization of a cost function, which consists of the error between the predicted outputs and the desired outputs [3]. In the literature, several MPC schemes were applied in machine drives and power electronics converters [4], [5]. A multivariable control strategy based on MPC approach has been proposed for a DFIG-based wind turbine in [6]. Moreover, wind turbine systems using the MPC approach provide excellent performance.

In order to compensate the harmonic currents generated by the nonlinear load, which would cause the fluctuation of the active power and reactive power. A shunt active power filter (SAPF) is implemented between the DFIG and the nonlinear load. There are different control techniques in compensation of the disturbance currents. Some research papers present the PI current controllers for the control of SAPF have been treated in [7], [8], the main problem in the use of traditional PI current controller; it is not capable of controlling the harmonic current accurately due to the control delay. This drawback could divert the system of its optimal operation. This is why the control should be concerned about the optimization and improvement the dynamic performances of SAPF. For that, we referred to the use of the nonlinear model predictive control (NMPC). An interesting MPC strategy to solve this problem has been presented by [9]. Several investigations have been dedicated to MPC due to its performance and robustness to nonlinear systems with fast dynamics. Besides, it ensures a minimum distortion. The NMPC has received much attention and constitutes a very active field of research in recent years.

Owing to the ability to predict the required reference currents and to compensate the disturbance currents at different conditions, we use the nonlinear predictive controller (NPC) applied to SAPF; the optimal control law is obtained by the minimization of a cost function. The latter consists of the difference between the predicted output and the measured output. It is usually based on a priori knowledge of the process through a model [10], [11].
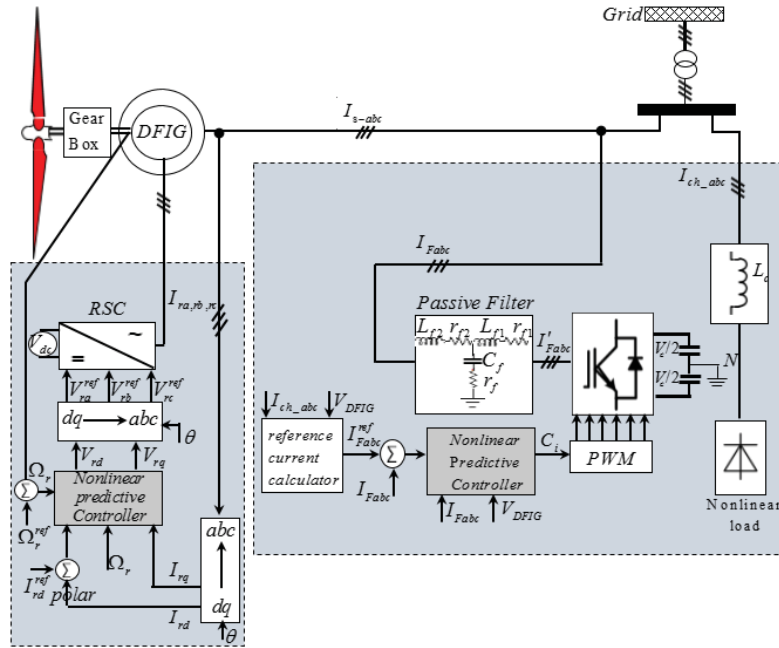

Fig. 1 Configuration of DFIG-based wind turbine with SAPF controlled by DNPC

In this paper, we focus on a nonlinear predictive control strategy. We propose a double nonlinear predictive controller (DNPC) to predict the required current references for SAPF, the required DFIG rotor current and the rotor speed references for DFIG respectively. The purpose of this strategy is to ensure the high-performance tracking of the rotor speed and regulate the rotor current of the DFIG. Thus, this strategy is to reject the harmonic currents generated by the nonlinear load and ensure that the stator voltage and stator current have a sinusoidal waveform.

II. DESCRIPTION OF THE SYSTEM STUDIED

The system to be studied is shown in Fig. 1; an AC-grid connection of DFIG-based wind turbine associated to an SAPF. It is constituted of the proposed connection of the DFIG-based wind turbine with SAPF. The whole system is controlled by DNPC. An SAPF is connected between the DFIG and the three-phase Diode Bridge supplied by a passive circuit (r_d, L_d). It can be observed that the DFIG rotor is controlled by RSC based on nonlinear predictive control strategy. The reference compensating currents are calculated by the reference currents calculator block, which is not addressed in this study. The nonlinear predictive controllers (NPCs) are used to predict the actual values of the output currents come from SAPF. As a result, the predictive values of the output currents are given by an optimal control law. This latter is obtained by minimizing a quadratic criterion,

including future error and future control values on a finite horizon prediction.

The SAPF is composed of a voltage inverter; it consists of three half-bridges based on IGBT transistors controlled by PWM [12]. The output filter is a passive filter used to connect the voltage inverter to the grid in order to respect the interconnection rules for the source. Moreover, the output filter is dimensioned to ensure a good dynamic of the shunt active filter current. Also, to mitigate the components due to the switching of the inverter from spreading into the grid. The voltage across the capacitor C is supposed continuously regulated.

III. MODELING OF THE WIND ENERGY CONVERSION SYSTEM

A. Model of the Turbine

The wind turbine used in this work, consists of a three blade wind turbine rotor with a radius R, driving a DFIG through a gain multiplier G. The wind power can be defined by:

$$P_v = \frac{\rho \cdot \pi \cdot R^2 \cdot v^3}{2} \qquad (1)$$

where, ρ : the air density, $\rho = 1.225\text{kg/m}^3$, R: the blade length, v: the wind speed. However, only part of the available energy can be captured by the wind turbine [13]:

$$P_v = \frac{\rho \cdot C_p \cdot \pi \cdot R^2 \cdot v^3}{2} \tag{2}$$

For wind turbines, the power coefficient C_p which depends on both of the wind speed and the rotational speed of the turbine is usually set in the range 0.35- 0.59 [14]. Thus, the DFIG transforms the rotational speed of the turbine into electrical energy.

B. Multiplier Model

The multiplier is disposed between the rotor wind turbine and the DFIG, is designed to adapt the turbine speed Ω_t, to that of the generator Ω_r. This multiplier is modeled by:

$$T_g = \frac{T_{aero}}{G} \tag{3}$$

$$\Omega_t = \frac{\Omega_r}{G} \tag{4}$$

with, G is the multiplier coefficient. In order to establish the evolution of the mechanical speed from mechanical torque, we apply the fundamental equation of the dynamics:

$$J_t \cdot \frac{d\Omega_r}{dt} = T_{mec} = T_g - T_e - f_r \cdot \Omega_r \tag{5}$$

with, Ω_r: mechanical speed of DFIG, T_e: electromagnetic torque, f_r: coefficient of friction.

C. Mathematical Model of DFIG

The modeling of DFIG is described in the referential Park. The following equation describes the modeling of the generator:

$$\begin{cases} V_{sd} = R_s I_{sd} + \dfrac{d}{dt}\psi_{sd} - \omega_s \psi_{sq} \\[2mm] V_{sq} = R_s I_{sq} + \dfrac{d}{dt}\psi_{sq} + \omega_s \psi_{sd} \\[2mm] V_{rd} = R_r I_{rd} + \dfrac{d}{dt}\psi_{rd} - (\omega_s - \omega_r)\psi_{rd} \\[2mm] V_{rq} = R_r I_{rq} + \dfrac{d}{dt}\psi_{rq} + (\omega_s - \omega_r)\psi_{sd} \end{cases} \tag{6}$$

with

$$\omega_r = p \cdot \Omega_r \tag{7}$$

$$\begin{cases} \psi_{sd} = L_s I_{sd} + L_m I_{rd} \\ \psi_{sq} = L_s I_{sq} + L_m I_{rq} \\ \psi_{rd} = L_r I_{rd} + L_m I_{sd} \\ \psi_{rq} = L_r I_{rq} + L_m I_{sq} \end{cases} \tag{8}$$

where R_s, R_r, are the resistance of the stator winding and resistance of the rotor winding respectively. $V_{s\text{-}dq}$, $V_{r\text{-}dq}$, $I_{s\text{-}dq}$, $I_{r\text{-}dq}$, $\psi_{s\text{-}dq}$, $\psi_{r\text{-}dq}$ are respectively the components of the stator and rotor voltages, stator and rotor currents, stator and rotor

fluxes represented in *dq* axis. ω_s, ω_r represents respectively stator and rotor angular velocities. p is the pole pairs number. L_m is mutual inductance, L_s, and L_r are stator self-inductance and rotor self-inductance. The electromagnetic torque is also expressed as a function of currents and flux by:

$$T_{em} = p\frac{L_m}{L_s}\left(\psi_{sq} I_{rd} - \psi_{sd} I_{rq}\right) \tag{9}$$

To easily control the production of electricity from a wind turbine, we shall realize independent control of active and reactive power by establishing the equations which bind the rotor voltage values to the stator active and reactive power [15]. For evident reasons of simplification, a *dq* reference related to the rotating field with stator flux aligned along the *d-axis* is adopted. Therefore, (8) of the flux becomes:

$$\begin{cases} \psi_{sd} = L_s I_{sd} + L_m I_{rd} = \psi_s \\ \psi_{sq} = L_s I_{sq} + L_m L_{rq} = 0 \end{cases} \tag{10}$$

If we assume that the grid is stable, this will lead to a constant stator flux ψ_s. Moreover, the stator resistance can be neglected. Based on these considerations, we get:

$$\begin{cases} V_{sd} = 0 \\ V_{sq} = V_s = \omega_s \psi_s \end{cases} \tag{11}$$

Using (10), we can establish the link between the stator and rotor currents:

$$\begin{cases} I_{sd} = \dfrac{\psi_s - L_m}{L_s} I_{rd} \\[3mm] I_{sq} = -\dfrac{L_m}{L_s} I_{rq} \end{cases} \tag{12}$$

The generator active and reactive powers are given by:

$$\begin{cases} P = \dfrac{3}{2}\left(V_{sd} I_{sd} + V_{sq} I_{sq}\right) \\[3mm] Q = \dfrac{3}{2}\left(V_{sq} I_{sd} - V_{sd} I_{sq}\right) \end{cases} \tag{13}$$

The adaptation of these equations to the simplifying assumptions gives

$$\begin{cases} P = -\dfrac{3}{2}\dfrac{V_s L_m}{L_s} I_{rq} \\[3mm] Q = \dfrac{3}{2}\dfrac{V_s}{L_s}\left(\psi_s - L_m I_{rd}\right) \end{cases} \tag{14}$$

By substituting (10) and (11) in (6) and (8), the *dq*-axis components of the armature rotor voltages are defined as:

$$\begin{cases} V_{rd} = R_r I_{rd} + \sigma L_r \dfrac{dI_{rd}}{dt} - \sigma L_r s\omega_s I_{rq} \\[3mm] V_{rq} = R_r I_{rq} + \sigma L_r \dfrac{dI_{rq}}{dt} - \sigma s\omega_s I_{rd} + s\omega_s \dfrac{L_m \psi_s}{L_s} \end{cases} \tag{15}$$

with

$$\sigma = 1 - \frac{L_m}{L_s L_r} \quad ; \quad s = \frac{\omega_s - \omega_r}{\omega_s}$$

s is the generator slip.

IV. MODELING OF THE SAPF

The SAPF consists of a voltage inverter based on IGBT transistors. We define the vector control of the switches states $T_1 \ldots T_6$ by:

$$[C] = [C_1 \quad C_2 \quad C_3] \qquad (16)$$

where (C_1, C_2, C_3) presents the switching function with:

$$\begin{cases} C_i = 1 \quad \text{for } T_i \ \text{closed} \\ C_i = 0 \quad \text{for } T_i \ \text{open} \end{cases} i \in \{1,2,3\}$$

The voltage vector of the active filter inverter relative to the neutral is given as:

$$[V_F] = [V_{Fa-N} \quad V_{Fb-N} \quad V_{Fc-N}] \qquad (17)$$

The relationship between the vector control and the vector voltages relative to the neutral is expressed as [16]:

$$[V_F]^T = \frac{V_c}{2} \cdot I_{(3 \times 3)} \cdot [C]^T \qquad (18)$$

with, $I_{(3 \times 3)}$ the identity matrix, V_C: the reduced effective value of the capacitor voltage.

The model of SAPF in single phase system can be expressed in the bilinear form [17]:

$$\begin{cases} L_{f_2} \dfrac{dI_F}{dt} = v_{cf} - v_{s\_DFIG} - r_{f_2} I_F \\ L_{f_1} \dfrac{dI'_F}{dt} = v_F - v_{cf} - r_{f_1} I'_F \\ C_f \dfrac{dv_{cf}}{dt} = I'_F - I_F \\ v_F = \dfrac{V_c}{2} C \end{cases} \qquad (19)$$

with v_{cf} is the voltage across the capacitor C_f, L_{f1}, L_{f2}, r_{f1}, r_{f2} are respectively the inductances and internal resistances of the passive filter, I_F, $I_F{}'$ are respectively the compensation currents of SAPF and output current of the inverter.

V. DOUBLE NONLINEAR PREDICTIVE CONTROLLER

A. Principle of Nonlinear Predictive Control

In this section, we will describe the basic principle for achieving nonlinear predictive control. The objective of the control is to determine, at every step sampling, the control sequence minimizing the error between the reference trajectory $y_r (t+\tau)$ and the predicted output $y (t+\tau)$ of the

system on the prediction horizon. It is defined by the cost function J which should be minimized.

$$J = \frac{1}{2} \int_0^{\tau_r} [y(t+\tau) - y_r(t+\tau)]^T [y(t+\tau) - y_r(t+\tau)] d\tau \quad (20)$$

where, τ_r: is the prediction horizon, $y (t+\tau)$: is the prediction of the output at τ step, $y_r (t+\tau)$: is the reference trajectory in the future.

To solve the cost function (20), the prediction of the outputs is made from the Taylor series expansion:

$$y_i(t+\tau) = h_i(x) + \sum_{k=1}^{\rho_i} \frac{\tau^k}{k!} L_f^k h_i(x) + \frac{\tau^{\rho_i}}{\rho_i!} L_{g_u} L_f^{(\rho_i-1)} h_i(x) u(t) \qquad (21)$$

The Lie derivative of function $h_i(x)$ along the vector field $f(x)$ is described by

$$\begin{cases} L_f h_i(x) = \dfrac{\partial h_i(x)}{\partial x} f(x) \\ L_f^k h_i(x) = L_f \left(L_f^{(k-1)} h_i(x) \right) \\ L_g L_f h_i(x) = \dfrac{\partial L_f h_i(x)}{\partial x} g(x) \end{cases} \qquad (22)$$

VI. DESIGN OF THE DOUBLE NONLINEAR PREDICTIVE CONTROLLER (DNPC)

A. Design the NPC of the DFIG

The aim of this controller is to ensure a perfect trajectory tracking of the rotor speed and to regulate the d-axis rotor current by acting on the rotor voltages. The model of DFIG in space form is given by using (5) and (15):

$$\begin{cases} \dot{x}(t) = f(x) + g_u u(t) + g_p T_{aero}(t) \\ y = h(x) \end{cases} \qquad (23)$$

where

$$x = [I_{rd} \quad I_{rq} \quad \Omega_r]^T \; ; \; u = [V_{rd} \quad V_{rq}]^T \; ; \; g = [g_d \quad g_q]$$

$$y = [I_{rd} \quad \Omega_r]^T$$

x, u, y, are respectively the state vector of the components of the armature rotor currents represented in dq frame and rotor speed, the input vector of the components of the armature rotor voltages in dq frame, and the system outputs, while $f(x)$, g_u, and g_p are described as:

$$f(x) = \begin{bmatrix} f_1(x) \\ f_2(x) \\ f_3(x) \end{bmatrix} = \begin{bmatrix} -\dfrac{R_r}{\sigma L_r} I_{rd} + s\omega_s I_{rq} \\ -\dfrac{R_r}{\sigma L_r} I_{rq} - s\omega_s I_{rd} + s\omega_s \dfrac{L_m \psi_s}{\sigma L_r L_s} \\ -\dfrac{f_r}{J} \Omega_r + \dfrac{1}{J} T_{em} \end{bmatrix}$$

$$g_u = \begin{bmatrix} \dfrac{1}{\sigma L_r} & 0 \\ 0 & \dfrac{1}{\sigma L_r} \\ 0 & 0 \end{bmatrix} \quad ; \quad g_p = \begin{bmatrix} 0 \\ 0 \\ -\dfrac{1}{J} \end{bmatrix} \tag{24}$$

We define the following output variables as d-axis component of the rotor current and the rotor speed as the variables to be controlled.

$$\begin{cases} y_1 = h_1(x) = I_{rd} \\ y_2 = h_2(x) = \Omega_r \end{cases} \tag{25}$$

The relative degree ρ_1 and ρ_2 of the outputs $y_1(I_{rd})$ and $y_2(\Omega_r)$ are equal to 1 and 2 respectively; they represent the order of its derivatives where we obtain the input u. Consequently, the relative degree of the DFIG outputs is equal to 3.

The optimal solution is obtained by derivation of the cost function with respect to control.

$$\frac{dJ}{du} = 0 \tag{26}$$

The resulting control law of the proposed NPC applied to the DFIG is given by:

$$u(t) = -G_u^{-1}(x)\left(\begin{bmatrix} \sum\limits_{i=0}^{1} K_i^1\left(L_f^i h_1(x) - y_{1r}^{(i)}(t)\right) \\ \sum\limits_{i=0}^{2} K_i^2\left(L_f^i h_2(x) - y_{2r}^{(i)}(t)\right) \end{bmatrix} + L_p(x)T_{aero}\right) \tag{27}$$

with

$$\begin{cases} K_0^1 = \dfrac{3}{2\tau_r}; K_1^1 = 1 \\ K_0^2 = \dfrac{10}{3\tau_r^2}; K_1^2 = \dfrac{5}{2\tau_r}; K_2^2 = 1 \end{cases}$$

$$G_u(x) = \begin{bmatrix} \dfrac{1}{\sigma L_r} & 0 \\ 0 & \dfrac{T_{em}}{JL_r} \end{bmatrix} \quad L_p(x) = \begin{bmatrix} 0 \\ -\dfrac{1}{J}K_1^2 + \dfrac{f_r}{J^2} \end{bmatrix}$$

B. Design the NPC of the SAPF

According to the expression of the SAPF in single phase (9) and as shown in [17], [18] the model of the SAPF in the space state form is given as

$$\begin{cases} \dot{x}(t) = f(x) + g_u u(t) + g_p p(t) \\ y = h(x) \end{cases} \tag{28}$$

with

$$x = \begin{bmatrix} I_F' & v_{cf} & I_F \end{bmatrix}^T \; ; \; u = C \; ; \; p = V_{s-DFIG} \; ; \; y = I_F$$

where x, u, p, y, are respectively the state vector, the control voltage, the measurable disturbance and the system output while $f(x), g_u$, and g_p are expressed as:

$$f(x) = \begin{bmatrix} -\dfrac{r_{f1}}{L_{f1}}I_F' - \dfrac{1}{L_{f1}}v_{cf} \\ \dfrac{1}{C_f}I_F' - \dfrac{1}{C_f}I_F \\ \dfrac{1}{L_{f2}}v_{cf} - \dfrac{r_{f2}}{L_{f2}}I_F \end{bmatrix} ; g_u = \begin{bmatrix} \dfrac{V_c}{2}\dfrac{1}{L_{f1}} \\ 0 \\ 0 \end{bmatrix} ; g_p = \begin{bmatrix} 0 \\ 0 \\ -\dfrac{1}{L_{f2}} \end{bmatrix}$$

The input relative degree ρ of the output y (i_F) is equal to 3. Consequently, it is equal to the system order, then the problem of the dynamics zero (unobservable states) no longer arises [19]. The optimal solution is obtained by using (26), then we obtain the optimal control input defined as follow:

$$u(t) = -G_u^{-1}(x)\left(\left[\sum\limits_{i=0}^{3} K_i^3\left(L_f^i h(x) - y_r^{(i)}(t)\right)\right] + L_p(x)p\right) \tag{29}$$

where

$$K_0^3 = \frac{21}{2\tau_r^3}; \; K_1^3 = \frac{42}{5\tau_r^2}; \; K_2^3 = \frac{7}{2\tau_r}; \; K_3^3 = 1$$

$$G_u(x) = \frac{1}{2} \cdot \frac{V_c}{C_f L_{f_1} L_{f_2}}$$

$$L_p(x) = \left(-\frac{42}{5\tau_r^2} + \frac{7r_{f_2}^2}{L_{f_2}} + \frac{1}{C_f L_{f_2}} - \left(\frac{r_{f_2}}{L_{f_2}}\right)^2\right) \cdot \frac{1}{L_{f_2}} V_{s-DFIG}$$

VII. COMPUTER SIMULATIONS

The computational simulation is conducted using the environment *MATLAB/SIMULINK* to validate the tracking performance of the proposed NPC applied to the DFIG, thus to tested the NPC applied to the SAPF that has the aim of predicting the currents references for SAPF and compensate individually or jointly, the disturbing currents generated by the nonlinear load. The main system parameters are listed in Table I. The predictive timer τ_r is set to 5 ms.

Fig. 2 presents a comparison between the actual output values of the SAPF current and its reference values, with the implementation of the NPC in the scenario of the control system. It should be pointed out that the SAPF is implemented to the control system at t = 0.02s. The NPC acted perfectly and accurately to estimate all the values of the SAPF current. Also, it is noticeable that the actual value of the output current tracks the desired trajectory. Of course, this due to the fact that the nonlinear prediction technique decreases the uncertainties between the actual output currents and its references. All we have said tends to demonstrate that the nonlinear predictive controller applied to the SAPF

ensures the high tracking performance of the current references. Contrary to the classical PI controller which cannot precisely track the reference values of the output currents.

TABLE I
PARAMETER VALUES OF THE DFIG AND SAPF

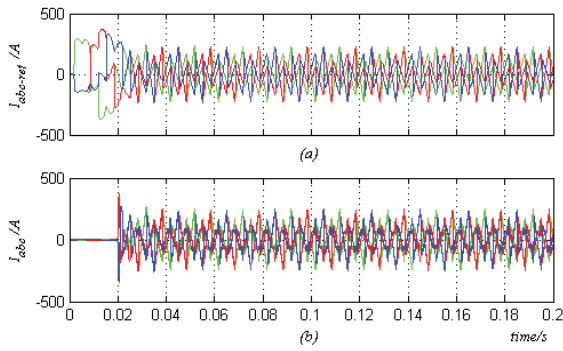| Designations	Codes	Values
$L_{f1} - r_{f1}$	Output filter of SAPF	300 mH – 1 Ω
$L_{f2} - r_{f2} \; C_f - r_f$		300 mH – 1 Ω
		150 µF – 0.5 Ω
$V_{c0}-C_0$	Supply DC of SAPF	640 V – 8.8 mF
V_{nom}	Rated voltage	380 V
f_{nom}	Rated frequency	50 Hz
P_{nom}	Rated power	1560 kW
n_{nom}	Rated speed	1500 rpm
p	Number of pole pairs	2

Fig. 2 Trajectory tracking of the output current for SAPF with NPC applied

Fig. 3 represents the temporal analysis of the DFIG-based wind turbine connected to the SAPF. This latter is implemented to the control system at t = 0.02s. One has to emphasize that the rotor speed is chosen equal to 0.85 per unit. By observing Fig. 3, it shows us that the actual speed of the rotor tracks its reference value. It can be seen that the DFIG stator voltage and current become sinusoidal waveform. This can be explained a good response provided by the SAPF based on NPC and an efficient of the NPC strategy applied to the DFIG. The DC voltage V_{dc} on the nonlinear load is stable around 850V. The DFIG active power in per unit is equal to 0.9, while the reactive power in per unit is equal to 0.3.

Fig. 4 summarizes the dynamic response of the system in permanent operating with DNPC applied to the DFIG and SAPF. The results proved a satisfying compensation for the disturbance currents and a good performance tracking of the rotor speed thus, for active and reactive power. One has to emphasize that the rotor speed in this simulation is considered variable its value changes between 0.85 and 1.2 per unit. What we find remarkable about this DNPC is that the performance of the system is guaranteed, even though the rotor speed of DFIG varies through time. All this goes to prove that the proposed AC-grid connection of DFIG-based

wind turbine with SAPF controlled by DNPC is appropriate for the variable speed machine operating.
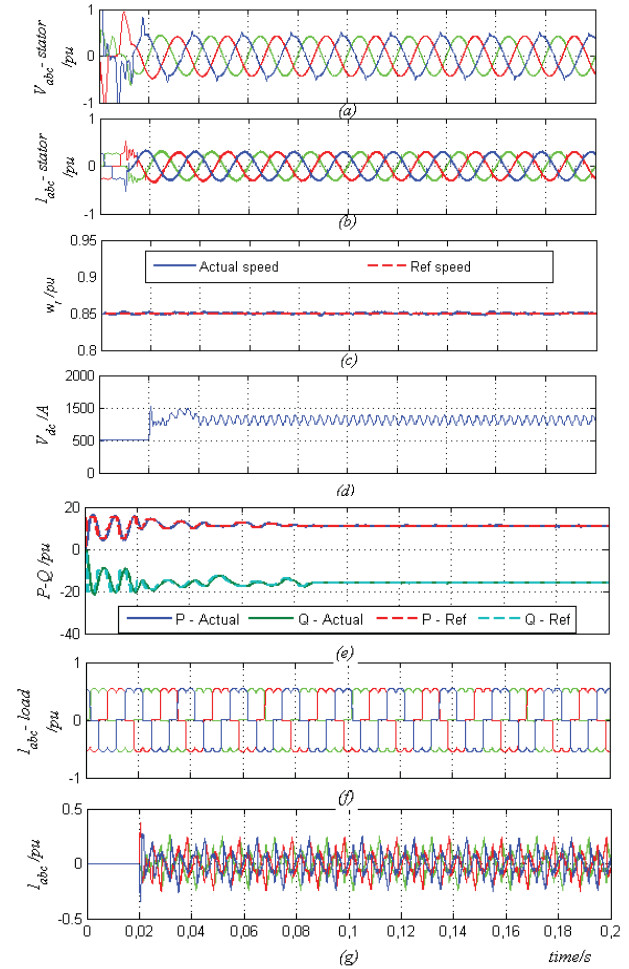

Fig. 3 Temporal analysis of DFIG systems with ω_r constant, (a) stator voltage of DFIG; (b) stator current of DFIG; (c) rotor speed; (d) DC load voltage; (e) active and reactive power of DFIG trajectory tracking; (f) AC-side current of the nonlinear load; (g) output current of the SAPF

Fig. 5 illustrates the harmonic spectrum of the stator current. It can be seen that the total harmonic distortion (THD) is acceptable according to limits imposed by the international standardization [12].

VIII. CONCLUSION

A double nonlinear predictive controller (DNPC) applied to the DFIG-based wind turbine connected to SAPF have been presented. The DNPC have been designed to predict the required currents reference for SAPF and required rotor speed value thus, the control of rotor current for DFIG. The optimal control laws of the DNPC are obtained from solving the optimization problems of the cost functions, which comprise the difference between the predicted outputs and the measured outputs over a fixed horizon.

Based on the computational simulation results, the predictive control laws implemented in the control of the DFIG and SAPF ensure the performance tracking. Also, reveal a good compensation of disturbance currents produced by the nonlinear load.
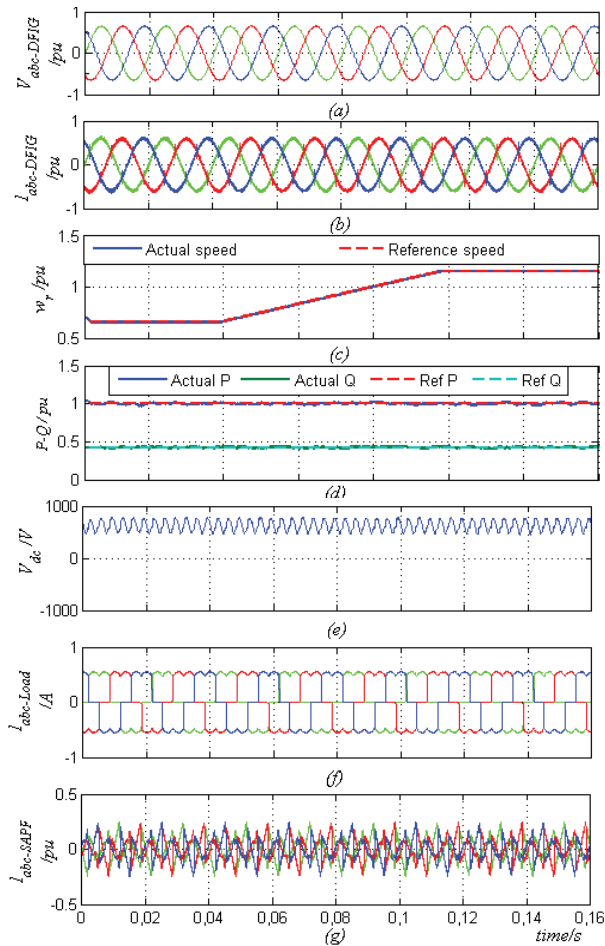

Fig. 4 Results of the dynamic response of DFIG system with ω_r change its value from 0.65 to 1.2. (a) stator voltage of DFIG; (b) stator current of DFIG; (c) rotor speed; (d) active and reactive power of DFIG trajectory tracking; (e) DC load voltage; (f) Ac-side current of the nonlinear load; (g) output current of SAPF
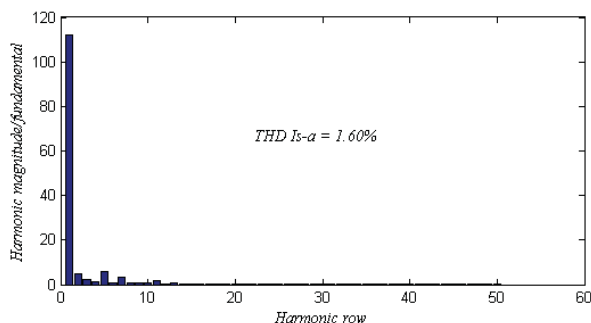

Fig. 5 Harmonic spectrum and THD of the current delivered by an NPC

REFERENCES

[1] G. O. Young, "Synthetic structure of industrial plastics (Book style with paper title and editor)," in *Plastics*, 2nd ed. vol. 3, J. Peters, Ed. New York: McGraw-Hill, 1964, pp. 15–64.
[2] W.-K. Chen, *Linear Networks, and Systems* (Book style). Belmont, CA: Wadsworth, 1993, pp. 123–135.
[3] H. Poor, *An Introduction to Signal Detection and Estimation*. New York: Springer-Verlag, 1985, ch. 4.
[4] B. Smith, "An approach to graphs of linear forms (Unpublished work style)," unpublished.
[5] E. H. Miller, "A note on reflector arrays (Periodical style—Accepted for publication)," *World Academy of Science, Engineering and Technology Trans. Antennas Propagat.*, to be published.
[6] J. Wang, "Fundamentals of erbium-doped fiber amplifiers arrays (Periodical style—Submitted for publication)," *World Academy of Science, Engineering and Technology J. Quantum Electron.*, submitted for publication.
[7] C. J. Kaufman, Rocky Mountain Research Lab., Boulder, CO, private communication, May 1995.
[8] Y. Yorozu, M. Hirano, K. Oka, and Y. Tagawa, "Electron spectroscopy studies on magneto-optical media and plastic substrate interfaces (Translation Journals style)," *World Academy of Science, Engineering and Technology Transl. J. Magn.Jpn.*, vol. 2, Aug. 1987, pp. 740–741 (*Dig. 9th Annu. Conf. Magnetics* Japan, 1982, p. 301).
[9] M. Young, *The Techincal Writers Handbook*. Mill Valley, CA: University Science, 1989.
[10] J. U. Duncombe, "Infrared navigation—Part I: An assessment of feasibility (Periodical style)," *World Academy of Science, Engineering and Technology Trans. Electron Devices*, vol. ED-11, pp. 34–39, Jan. 1959.
[11] S. Chen, B. Mulgrew, and P. M. Grant, "A clustering technique for digital communications channel equalization using radial basis function networks," *World Academy of Science, Engineering and Technology Trans. Neural Networks*, vol. 4, pp. 570–578, July 1993.
[12] R. W. Lucky, "Automatic equalization for digital communication," *Bell Syst. Tech. J.*, vol. 44, no. 4, pp. 547–588, Apr. 1965.
[13] S. P. Bingulac, "On the compatibility of adaptive controllers (Published Conference Proceedings style)," in *Proc. 4th Annu. Allerton Conf. Circuits and Systems Theory*, New York, 1994, pp. 8–16.
[14] G. R. Faulhaber, "Design of service systems with priority reservation," in *Conf. Rec. 1995 World Academy of Science, Engineering and Technology Int. Conf. Communications,* pp. 3–8.
[15] W. D. Doyle, "Magnetization reversal in films with biaxial anisotropy," in *1987 Proc. INTERMAG Conf.*, pp. 2.2-1–2.2-6.
[16] M. Prodanovic, T.C. Green, "Control and filter design of three-phase inverters for high power quality grid connection," IEEE Transactions on Power Electronics, vol. 18, pp. 373-380, January 2003.
[17] T. Jarou, A. El Kachani, N. El Haj, A. Niaaniaa, "New Control Based on Estimated State Feedback of the Shunt Active Filter to Compensate for the Disturbing Currents in the Electric Power," International Review on Modelling and Simulations (IREMOS), vol. 7, pp. 457-465, June 2014.
[18] C.-T. Chen, Linear system theory and design, Holt, Rinehart, and Winston, 1984.
[19] A. Isidori, Nonlinear Control Systems, Springer-Verlag, London, 1995, pp. 162-171.

Abderrahmane El Kachani is currently a Ph.D. student in Electrical Engineering within LHESIR laboratory, Physics department at Ibn Tofail University in Morocco. He graduated a Master of Science and Technology in Automatic and Industrial Informatics and a Bachelor of Science and Technology in Electronic Electrical and Automatic at the Faculty of Science and Technology Settat. Abderrahmane worked several years on industrial automation at the company "Cellulose Du Maroc" before starting his research studies focused on the electric power sources based on energy renewable and Active Power filters.

El Mahjoub Chakir is a professor of nuclear physics. He received Doctorate degree in nuclear physics from University Mohamed V, Rabat, Morocco, on 12th April 1994. He is a member of the research Laboratory of High Energy, Engineering Sciences and Reactors (LHESIR) Univ. Ibn Tofail, Faculty of Sciences, Kenitra. He is the supervisor of several Ph.D. Thesis. The author of several scientific publications.

Anass Ait Laachir is currently a Ph.D. student in Electrical Engineering within LHESIR laboratory, Physics department at Ibn Tofail University in Morocco. He graduated a Master degree in Microelectronics at Ibn Tofail University. His main area of research includes quality of electrical energy, Active Power filters and the electric power sources based on renewable energy.

Abdelhamid Niaaniaa is currently a Ph.D. student in Electrical Engineering within LHESIR laboratory, Physics department at Ibn Tofail University in Morocco. He graduated an Engineer Diploma in Electrical Engineering option Microelectronics at the National School of Applied Sciences in 2011 from the University Mohamed Premier (Oujda). He currently holds the position uploaded Engineer & Technical Sales business in CIETEC (Crossroads Industrial and technological). His main research focuses on Hybrid Systems Renewable Energy Sources with the aim and achieves optimal supervision of these sources.

Jamal Zerouaoui is a professor of Analytical mechanics and head of the Laboratory of High Energy, Engineering Sciences and Reactors (LHESIR) Univ. Ibn Tofail, Faculty of Sciences, Kenitra. He is Supervisor of several Ph.D. Thesis. The author of several scientific publications.

Tarik Jarou is currently a professor at the National School of the Sciences Applied of the University Ibn Tofail, Kenitra, Morocco. He received Doctorate degree in Electric Engineering from the Engineer School Mohammedia of the University Mohamed V, Rabat, Morocco. He is a member of the research laboratory LHESIR of the University Ibn Tofail. His main area of research includes the modeling and the control of electric systems control, the supervision of electric power sources with energy renewable and the implementation of the algorithms on the embedded systems.